Carbon Dynamics on the Molybdenum Carbide Surface during Catalytic Propane Dehydrogenation

Benjamin Frank,[a] Thomas P. Cotter,[a,b] Manfred E. Schuster,[a] Robert Schlögl,[a] and Annette Trunschke*[a]

Abstract: Mesoporous bulk molybdenum carbide has been investigated as a catalyst for propane dehydrogenation to propylene. A surface-sensitive study by means of in situ XPS and Raman techniques evidences that the dynamic formation/removal of surface coke strongly shifts the product spectrum to the desired C_3-alkene, that is, away from low-value hydrogenolysis products. A similar response of selectivity, which is accompanied by a boost of activity, can be achieved by tuning the oxidation state of Mo by reaction process parameters as well as by V doping. Results obtained allowed us to draw a picture of the active catalyst surface and to propose a structure-activity correlation as a map for catalyst optimization.

Keywords: oxycarbide • coking • deactivation • selectivity • oxidation state

Introduction

Since the early transition metal carbides were found to provide noble metal-like properties,[1,2] there has been a renewed interest in these materials in the field of catalysis, especially so in the case of group V and VI carbides. It is hoped that such materials may be able to substitute scarcer and more expensive noble metals in a growing field of applications, including fuel cells and energy-related catalysis. The direct dehydrogenation (DH) of light alkanes is of permanently high interest in chemical industry and reported over bulk and supported molybdenum carbide and oxycarbide for ethane,[3] propane,[4,5] and butane.[6–10] The relatively low number of studies concerning this topic reflects the difficulties associated with these reactions, namely severe deactivation, a complex reaction network, and the dynamic nature of the carbide surface. Literature on catalytic propane DH is dominated by supported Cr oxides[11] and Pt-based systems.[12] However, these catalysts are either rare and costly, or hazardous. Sn, especially in the combination with platinum as Pt-Sn/Al_2O_3 is one of the most popular promotors.[12] However, also Cu-based catalysts provided a surprisingly high propylene productivity even at low temperatures.[13]

Solymosi *et al.* report on propane DH over bulk and supported Mo_2C as well as the influence of CO_2.[4,5] In the dry feed bulk Mo_2C predominantly produces propylene ($S = 44\%$) with the byproducts CH_4 and ethylene. Supported Mo_2C/SiO_2 shows a higher propylene selectivity. A strong impact of the dynamics of surface oxygen and carbon, however, is evidenced by the initial selectivity to propylene of the *in-situ* prepared silica supported catalyst, which is zero and increases with time on stream. Contrarily, the passivated (surface-oxidized) bulk catalyst is initially selective to propylene.

The reactions of *n*-butane over Mo oxycarbide have been extensively studied by Ledoux *et al.*,[6,10,14] who describe a carbon-modified MoC_xO_y phase being selective to C_4 olefin products in a $H_2/C_4H_{10}/H_2O$ feed. Reduction of the H_2O content leads to reduction of the oxycarbide and increasing selectivity to hydrogenolysis. A comparative study by Thompson *et al.*[7] contrasts the relative product selectivities in butane activation over the group V and VI transition metal carbides. For Mo_2C, the selectivities to DH, isomerization, and hydrogenolysis are 62, 4, and 34%, respectively. This appears incommensurate with the findings of Ledoux *et al.*, however, the temperature-programmed reduction-carburization (TPRC) stopped at 660°C and H_2 pretreatment of the passivated sample was carried out at 480°C. Under these conditions the carburization is likely incomplete and bulk oxygen, which is mobilized under the reaction conditions applied, will form an oxycarbide overlayer. It is also observed that the vanadium carbide materials were highly active for butane DH.

We recently reported on the large-scale preparation of well-defined mesoporous hcp β-Mo_2C as well as the impact of its V doping (3 to 11%).[15] CNT-supported systems have also been investigated in methanol steam reforming[16] or higher alcohol synthesis.[17] The present work concerns the performance of the bulk catalysts in propane activation including a detailed analysis of the

[a]   Dr. B. Frank, Dr. T. P. Cotter, Dr. M. E. Schuster, Prof. Dr. R. Schlögl, Dr. A. Trunschke
        Department of Inorganic Chemistry
        Fritz-Haber-Institut der Max-Planck-Gesellschaft
        Faradayweg 4-6, D-14195 Berlin, Germany
        Fax: (+) 49 30 8413 4457
        E-mail: trunschke@fhi-berlin.mpg.de

[b]   Dr. T. P. Cotter (present address)
        Clariant Int. AG
        Waldheimer Str. 13, 83052 Heufeld, Germany

        Supporting information for this article is available on the WWW under
        http://www.chemeurj.org/ or from the author.

active surface. A conceptually different motivation arises from the question as to whether the reducing gas mixture obtained in typical selective oxidation processes over, *e.g.*, Mo/V mixed oxide catalysts beyond full O_2 conversion could lead to the formation of carbide phases, at least near the reactor outlet. Thus, as the oxidation state of Mo controls its catalytic performance, the oxidative chemical potential of the reactant mixture was systematically varied by adding O_2, H_2O, and CO_2 to the $C_3H_8/H_2/N_2$ feed.

Results and Discussion

Reactivity in propane dehydrogenation: Catalytic experiments on the undoped β-Mo_2C reveal that the critical temperature for stable operation conditions in the oxygen-free feed is in between 500-550°C (Fig. 1). Here, equilibrium conversions of propane DH range from 20-30%.[18] Although the carbide phase is stable, heavy coke formation leads to a rapid decrease in activity with time on stream at the higher temperatures. This adverse effect is also prominent on Pt- or Cr-based systems,[19] which, however, can easily regenerated by oxidation with air.[20] Propane conversions in our experiments are rather low (< 5%), however, the propylene productivity over β-Mo_2C in the pseudo-steady state is among the highest reported at 500°C (Fig. 1). Thus, mechanistic insight in coke formation might initiate strategies for the superior process design.
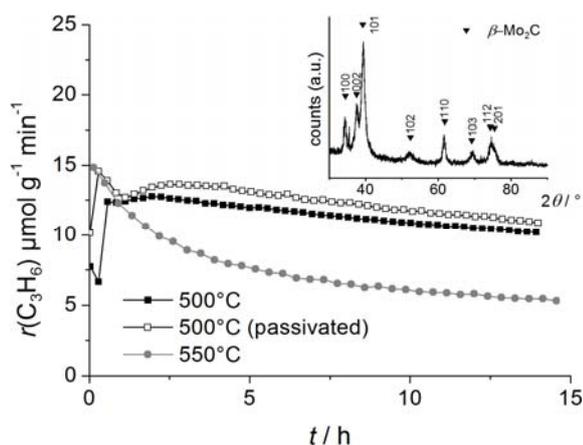

Figure 1. Reaction profiles of undoped β-Mo_2C in propane DH ($C_3H_8/H_2/N_2$ = 1:2:1). Inset: XRD pattern of used sample.

The general product spectrum is indicative for propane DH to propylene and primary hydrogenolysis to CH_4 and C_2H_6 as the main reactions. CH_4 excess ($S_{CH4} > S_{C2Hx}$) points at the secondary ethane hydrogenolysis to CH_4, whereas C_2H_4 can be formed by both the DH of C_2H_6 and hydrogenolysis of propylene. Dominance of the latter is revealed by the S-X plot (see the Supporting Information, Fig. S1). Quite the opposite, increasing C_2H_6 selectivity points at the *hydrogenation* of C_2H_4, according to the 10 fold lower equilibrium constant of ethane DH and H_2 excess in the feed.[18] The latter, however, is a common strategy to reduce coke formation. These results nicely agree with moderate propylene selectivities obtained over freshly carburized Mo_2C and Mo_2C/SiO_2 catalysts.[4] Also over Pt-based catalysts a pronounced evolution of dehydrogenation selectivity is observed,[19] which can be likely referred to equilibration of carbon and oxygen species on the active catalyst surface.

Process of coke formation: The oxycarbide overlayer generated on as-prepared carbides by 0.5% O_2/He passivation is completely removed under the reaction conditions applied, as indicated by the initial formation of CO and H_2O, after which the catalytic performance of the passivated catalyst is identical to that of the as-prepared one (Fig. 1 and Fig. S2 in the Supporting Information). The process of coke formation on the catalyst surface can be followed by Raman spectroscopy, where typical bands located at 1360 and 1580 cm^{-1}, the so-called *D*- and *G*-bands,[21] indicate the presence of disordered and graphitic carbon, respectively. The as-prepared catalyst is free of these features, which confirms the optimized preparation process avoiding the formation of a coke overlayer by extended carburization.[15] At 500°C, weak bands slowly arise, whereas the catalyst used at 550°C is characterized by heavy coke deposition (Fig. 2). Similar observations are made on Pt-based catalysts.[19] However, the analysis in terms of *D*- and *G*-bands is too simplified as all (polymeric) species contribute their skeletal vibrations. This can be seen in the dynamics of deposition/-hydrogenation in the first 4 h (Figs. 1 and 2) and later by the fact that carbon deposition runs into a steady state despite continuous addition of potential feed molecules for soot formation. The large contribution of reaction conditions is seen in the massive profile change from in-situ to ex-situ coming from the fact that during isolation of the sample massive hydrogenation/deposition takes place and the ex-situ surface is covered by polymer/molecular film rather than by coke (see white coke and black coke in zeolites[22]). The cooling prevents dehydrogenation of initial molecular deposits. Regarding reactivity, it is evident, that coke formation and the dynamics of surface carbon affect the hydrogenolysis to CH_4 and C_2H_6 to a much larger extent than the selective DH (Fig. S2).
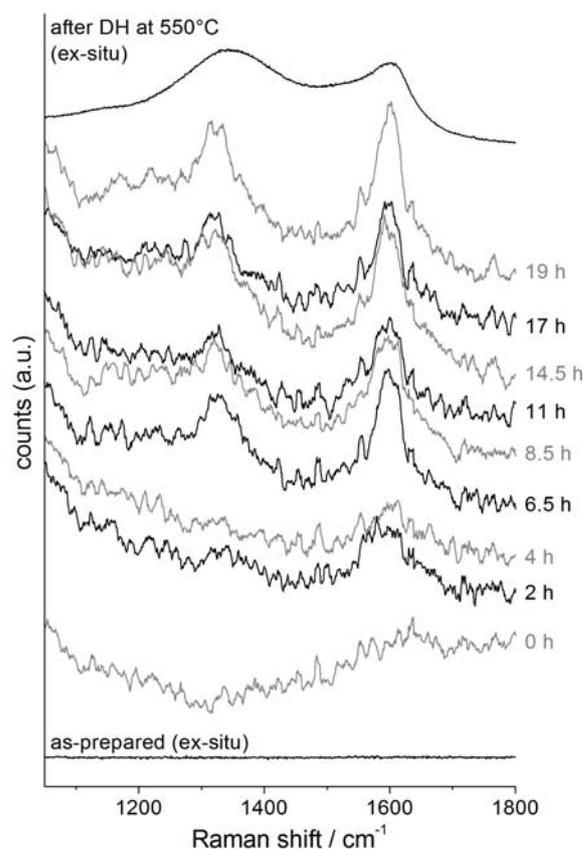

Figure 2. Quasi in-situ Raman analysis of *D*- and *G*-band evolution from carbon deposition during coke deposition at 500°C ($C_3H_8/H_2/N_2$ = 20/55/25). Bottom and top spectra show the ex-situ characterization of as-prepared β-Mo_2C and after use in propane DH at 550°C.

2

Dynamics of carbide phases: The penetration of surface carbon into the catalyst bulk was investigated by TPRC (T_{max} = 600°C) of hexagonal h-$Mo_{1-x}V_xO_3$ precursors with propane. Here, the fcc α-phase is formed (Fig. 3). Compared to CH_4,[15] longer-chain hydrocarbons lead to this thermodynamically unstable phase, as a consequence of weaker C-H bonds leading to a low phase transformation temperature. The evolution of CO as the indicator for bulk carburization begins at 450°C, proving the vital carbide formation and regeneration to be relevant under DH conditions applied. It supports healing of passivated Mo_2C under propane DH conditions (Fig. 1).
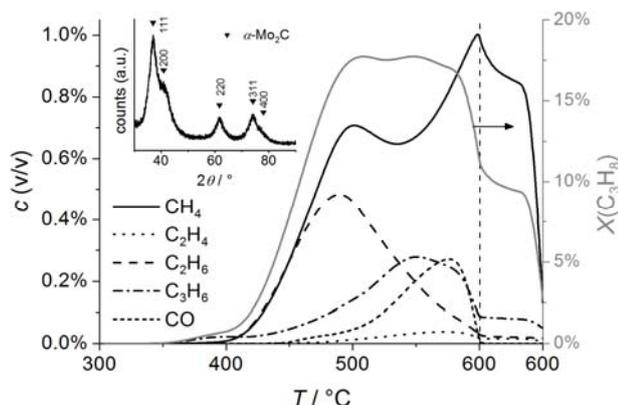

Figure 3. TPRC profile of h-MoO_3 in $C_3H_8/H_2/N_2$ = 25/55/20. Inset: XRD pattern of the resulting carbide.

The pronounced formation of hydrogenolysis products CH_4 and C_2H_6 peaking at 500°C points at partially reduced phases (MoO_2, MoO_xC_y) to be responsible for this side-reaction, whereas the formation of propylene increases with the release of CO, however, drops at full reduction of the catalyst due to rapid coking. A low-temperature shoulder (350-420°C) indicates that propylene is not only formed by DH on the freshly formed carbide phase but propane could also act as the reducing agent for Mo^{VI} via oxidative DH[23,24] yielding propylene and H_2O. Considering the mobility of O^{2-} this may explain the weak shift of C_3H_6 with respect to CO evolution curves (Fig. 3). This experiment impressively underlines the delicate balance of the Mo oxidation state required for selective DH catalysis.
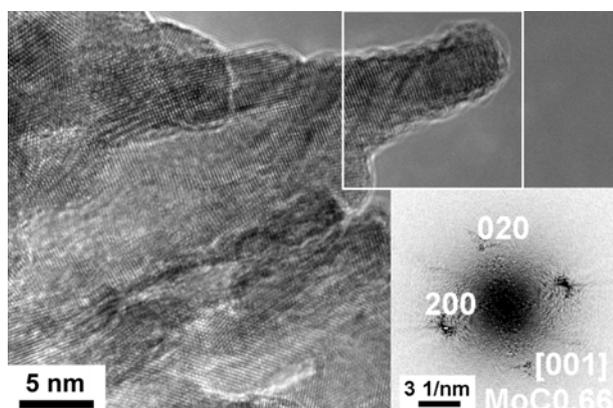

Figure 4. TEM image of a used Mo_2C catalyst. Inset: SAED of the selected area showing the α-MoC_{1-x} phase reconstruction.

Interestingly, the β-Mo_2C catalysts treated in $C_3H_8/H_2/N_2$ also contain small domains of metastable α-MoC_{1-x} (invisible by XRD), which could be identified in the HRTEM analysis by selected area electron diffraction (SAED) experiments (Fig. 4, inset). This phase was not detected on the fresh catalyst sample. Such cubic sub-domains appear to be integrated within the matrix of the bulk carbide and potentially come about *via* a high temperature recrystallisation of the surface oxycarbide layer.

The dynamics of surface O and C in carbide catalysts on the performance calls for a study on the stability and reactivity of Mo_2C under different oxidative potentials (Tab. 1). Post mortem X-ray diffraction (XRD) analyses after at least 10 h time-on-stream reveal that the carbide phase degenerates to MoO_2 and MoO_3 in case of either H_2O or O_2 addition to the C_3H_8/N_2 feed. However, resistance against H_2O can be achieved by adding H_2 to the gas mixture. In the presence of H_2O and CO_2 additional side-reactions can occur, namely steam reforming of propane and water-gas shift, which substantially lower the propene selectivities obtained. However, absolute propene productivities still exceed the pure propane feed by more than one order of magnitude. This can only in parts be referred to the beneficial effect of H_2.[25] It is evident that mild oxidants such as H_2O or CO_2, if phase stability is provided by additional H_2, can boost the catalyst activity either by improved coke removal or by tuning the oxidation state of Mo.

Table 1. Conversions (X) and propylene selectivities (S) of Mo_2C in propane DH depending on addition of potential oxidizing agents.[a]

Gas phase[b] / %					final	X /	S /	r_{C3H6} /
C_3H_8	H_2	H_2O	CO_2	O_2	phase	%	%	$\mu mol\ g^{-1}\ min^{-1}$
10	-	-	-	-	β-Mo_2C	0.1	100	0.6
25	50	-	-	-	β-Mo_2C	2.0	60.0	10.2
25	55	20	-	-	β-Mo_2C	12.9	13.6	14.9
10	-	10	-	-	MoO_2	1.0	95.3	5.4
25	55	-	20	-	β-Mo_2C	6.7	25.1	14.3
10	-	-	-	3.5	MoO_3	0.4	90.2	2.0

[a] 500°C, GHSV 8250 ml g^{-1} h^{-1} (10% C_3H_8) or 5000 ml g^{-1} h^{-1} (25% C_3H_8), after 10 h time on stream; [b] N_2 balance.

For comparison with the state-of-the-art catalyst systems for propane DH the following literature benchmarks are given: The propylene productivity over a 0.5% Pt/Al_2O_3 catalyst[19] at 600°C in 25% C_3H_8/H_2 is in the range of 20-40 $\mu mol\ g^{-1}\ min^{-1}$, strongly depending on the degree of deactivation, which, however, occurs on a significantly shorter time-scale than for bulk MoC at 500°C (Fig. 1). At the higher temperature, however, C_3H_8 conversion and C_3H_6 selectivity range from 15-50% and 15-70%, respectively, suggesting a superior suitability for economic process design. The C_3H_6 productivity increases after addition of a Sn promoter up to a level of 30-45 $\mu mol\ g^{-1}\ min^{-1}$.[19] Also, a 13% Cr/Al_2O_3 catalyst[26] at 550°C in 9% C_3H_8/He gives C_3H_6 productivities ranging from 70-120 $\mu mol\ g^{-1}\ h^{-1}$ at C_3H_8 conversions of 25-45%. Similarly to the MoC system, a partially reduced Cr^{3+}/Cr^{2+} state is discussed as the selective dehydrogenation site.[11]

Dynamics of electronic surface properties: We performed an *in situ* XPS study to clarify the origin of this promoting effect. Unfortunately, coke formation does not occur under low pressure conditions. Instead, surface (aliphatic) carbon is rapidly removed in pure H_2 at 600°C leaving a clean carbide surface with some residual

oxygen (see the Supporting Information, Fig. S3). The Mo_2C catalyst was subsequently cooled to 500°C and exposed to $C_3H_8/H_2/He$ (2:1:1). The surface of the carbide becomes progressively oxidized, which is due to the mobilization of residual oxygen in carbide bulk. This process coupled with the related product spectrum illustrates a valuable picture of surface reactivity with respect to surface oxidation. A selection of the Mo3d spectra as well as peak assignments and positions are shown in the Supporting Information (Fig. S4, Tab. S1). Still the reliable and accurate assignment of peaks in such a multi-component structure is very difficult. The complex electronic nature of Mo suboxides prevents their exact determination and instead attempts have been made to present a consistent pattern of fitting for the data that may be gauged against the observed reactivity.

Metallic Mo^0 and carbidic Mo^{II} peaks have been assigned to $3d_{5/2}$ features at around 227.8 and 228.3 eV, respectively. Mo^{IV} is divided into two separate species; the metallic screened (S) peak (metallic character; delocalized electrons) at 229.3 eV and a contribution from non-metallic unscreened (U) states (oxidic character; more localized electrons), which is observed as a broad doublet with 231 eV. Finally, a small feature at 232.7 eV is attributed to Mo^{VI} but this may also coincide with a shake-up peak of Mo^0 (227.8 + 5.1 eV).[27–31] The observed changes in surface oxidation are represented by the peak integrals plotted over time on stream (Fig. 5). The metallic and carbidic character of the surface is slowly oxidized over the first 3 h with a steadily growing contribution from Mo^{IV} (S). After 3-4 h the oxidation accelerates and results in a large increase in the Mo^{IV} (U) doublet. In parallel, the initial rate of C_3H_6 formation is high and drops as the formation rates of C_2H_4 and C_4H_8 rapidly increase within the first 2 h. Recombinative hydrocarbon formation products C_2H_4 and C_4H_8 are observed to decrease in parallel after 4-5 h. Apparently, the oxidation state of the surface is detrimental for the reaction switching between alkylidene recombination (metathesis) and dehydrogenation.
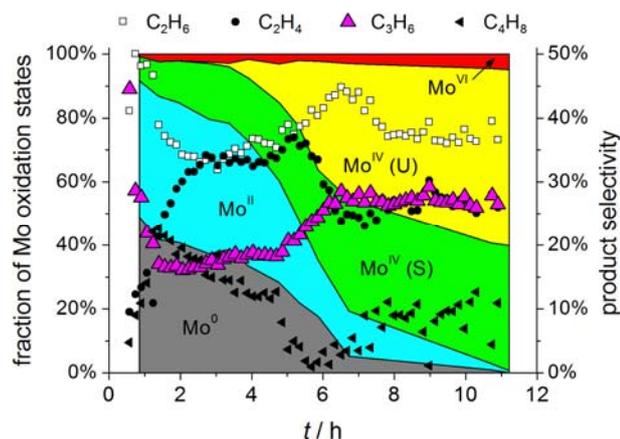

Figure 5. In situ XPS analysis: stacked area plot of Mo oxidation states overlaid with relative product distribution of propane DH in $C_3H_8/H_2/He$ (2:1:1) at 500°C.

The valence band (VB) spectra recorded during the *in situ* run (see the Supporting Information, Fig. S5) provide additional insight into the reaction mechanism. Throughout the reaction there is a significant electron occupation of the density of states (DOS) at the Fermi edge, implying that the system remains metallic. However, the VB spectra show a decreasing electronic density of states close

to the Fermi edge and an increase of intensity at around 6 eV binding energy. This valence band region is typically dominated by O2p states in transition metal oxides and thus reflects the progressing oxidation of the surface. In the final spectra it can be seen that the overlap between the Mo4d and O2p bands is strongly decreased to the point that the bands are almost discrete. The cross-sectional view through the VB spectra at binding energies of 0.5, 1.5, and 2.5 eV illustrate the electron density at the Fermi edge, the Mo4d state, and at the overlapping region between the 4d and O2p states, respectively. While the DOS at the Fermi edge remains unchanged, the electron density in the Mo4d VB decreases strongly from $t = 4$ to 6 h in concert with the observed formation of C_2H_4. Again, this is explained by an ongoing surface oxidation that reduces the number of Mo4d electrons in an ionic picture for metal oxides. While covalent bounding modifies the DOS Mo4d occupation, the general trend still holds. Moreover, the separation between the Mo4d and O2p states occurring from $t = 4$ h, is observed to coincide with the decrease in C_4H_8 formation rate. Thus the observed changes in the valence band region support the interpretation/assignment of the Mo3d core level spectra.

Although rapid water-gas shift[32] and consecutive steam refor-ming drastically alter the propane DH product spectrum towards less valuable compounds, the boosted propylene productivity in the presence of CO_2 (Tab. 1) calls for detailed surface analysis. A more reducing feed of $C_3H_8/H_2/CO_2 = 1:2:1$ was applied in the in situ XPS analysis, keeping the catalyst in reduced state. Unfortunately, due to problems with GC analysis (H_2/C_3H_6 overlap), only the CO, CO_2, and C_2H_4 traces could be extracted from the chromatograms. However, according to the ambient pressure catalytic experiment (Tab. 1, Supporting Information, Fig. S6) it can be assumed that the evolution C_2H_4 and C_3H_6 product formation goes in parallel.

The initial formation rate of C_2H_4 inversely decreases to the rate of CO formation *via* reverse water-gas shift (rWGS, Fig. 6a). This process coincides with a loss of oxygen (Fig. 6b). The O1s spectrum consists of a sharp line at around 530 eV describing structural oxygen and broad shoulders indicative for adsorbed and dissolved atomic oxygen species and OH groups. Different bond strengths of oxo- and carbo-species with respect to Mo in different oxidation states may be the driving force for structural dynamics and reactivity equilibration. In Fig. 6 the final O1s spectrum decreases slightly in intensity as rWGS appears to level off, and C_2H_4 formation further decreases. The Mo3d and C1s peaks are characteristic of the reduced Mo_2C throughout (not shown). Again, a detrimental impact of oxygen in the catalyst on its performance is indicated supporting the hypothesis that an oxygen-moderated carbide phase is more active for the dehydrogenation of alkanes.

Regarding the CO_2 co-feed it must be mentiond that a positive influence of this gas on propane DH has also been reported for a silica-supported Mo_2C catalysts.[5] Here, it was concluded that beyond 773 K CO_2 acts as the oxidizing agent to form a highly active and selective oxycarbide phase. This interpretation is supported by the present *in situ* XPS study performed on a bulk Mo_2C system.
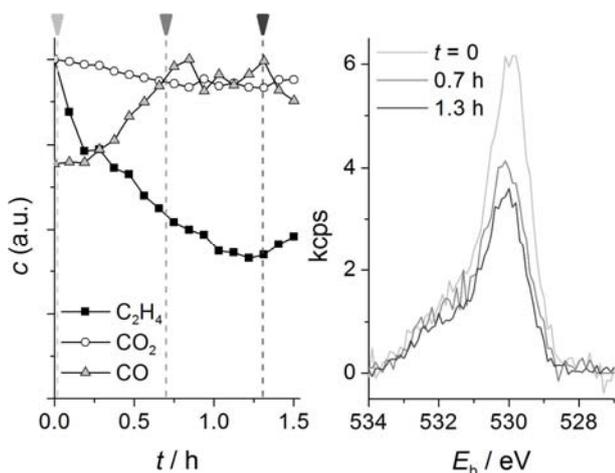
Figure 6. *In situ* XPS analysis of Mo_2C: (a) normalized product formation rates over time on stream in $C_3H_8/H_2/CO_2$ (2:1:1) at 500°C; (b) evolution of O1s peak with time on stream.

Impact of vanadium doping: The question arises how to stabilize an appropriate oxidation state of Mo avoiding the co-feed of H_2O or CO_2, which favor steam reforming pathways. We recently reported on the synthesis of mesoporous V doped Mo_2C materials[15] and it is well known that V exhibits a higher oxophilicity than Mo, thus could be an appropriate dopant in Mo/V binary carbide catalysts. The addition of V strongly influences the carburization temperature of the hexagonal h-$Mo_{1-x}V_xO_3$ precursors suggesting a stabilizing effect on redox properties of the materials. Here is an analogy to the Pt-Sn/Al_2O_3 system. The degree of the Sn reduction has been found to depend on the Sn loading, temperature of the pretreatment and the presence of surface additives such as chlorine.[33] Pt–Sn alloy phases in addition to oxidic tin states have been detected from in situ studies.[34] Thus, moderate doping with oxygen could also be a key factor for activity and selective dehydrogenation in this system.

Table 2. Physicochemical properties and catalytic performance of Mo/V carbides.

Sample	E_{kin} [a] / eV	β-Mo_2C	β-$(Mo_{0.92}V_{0.08})_2C$
V/Mo	150	-	0.4
	600	-	0.1
C/Mo	150	2.0	4.5
	600	0.7	1.1
O/Mo	150	2.8	5.1
	600	0.1	0.2
S_{BET} [c] / m^2 g^{-1}		25	34
r_{C3H6} [b] / μmol g^{-1} min^{-1}		10.2	18.0
$E_{a,app}$ / kJ mol^{-1}		80±3	88±4

[a] E_{kin} was varied for depth profiling. The inelastic mean free path in MoO_3 is approximately 0.6 and 1.4 nm for experiments performed at 150 and 600 eV, respectively; [b] 500°C, $C_3H_8/H_2/He$ = 1:2:1, GHSV = 5000 ml h^{-1} g^{-1}; [c] after catalytic test.

The *ex-situ* XPS analysis shows that the surface of the catalyst is rich in oxygen but remains in an overall reduction state below MoO_2. The spectra taken at higher kinetic energy indicate that the subsurface is predominantly carbidic. C1s spectra show two distinct maxima at E_b = 285 and 283.3 eV, which relate to surface carbon (C-C, C-H, C-O) and carbidic carbon, respectively. Depth profiling indicates that the surface is dominated by adventitious carbon, and that V doping leads to a larger contribution from associated carbon

and oxygen species at the surface (Tab. 2). Thus, oxygen is to a large extend associated to this surface carbon deposit (see the Supporting Information, Fig. S3) rather than being incorporated into the bulk. Notably, the surface V/Mo ratio of 0.4 in the carbide, which is only doped by 8 at.% V, suggests that the immediate surface layer is highly enriched in V. Here, also an increase in subsurface carbon is observed in comparison to the undoped Mo_2C. These observations suggest that the formation of the carbide has resulted in mobilisation of the V atoms towards the surface.

The qualitative analysis of the V2p spectrum indicates that the primary structure consists of a broad doublet centred at $3d_{5/2} \approx 515.8$ eV. Comparison with energies reported in the literature suggests that the V atom is in a reduced oxidation state such as found in V_2O_3.[35] Electron energy loss spectra (EELS) were obtained for the samples to give information about the chemical states of the elements present in the matrix. As can be seen in Figure S7 (see the Supporting Information), the Mo M edge is rather broad and has a small feature (M 4,5) at 227 eV and further features visible at 393 and 410 eV (M3 ,M2). A large peak was observed for the C K-edge, which is indicative of the presence of sp^2-bonded carbon that is in agreement with Raman spectra (Fig. 2). The final feature of note is the doublet peak observed at ca. 515 eV for the V L-edge. As was observed for the *ex situ* XPS the energy range of the $3d_{5/2}$ peak suggests that the vanadium is in an intermediate oxidation state (V^{3+}).

These observations can be related with the catalytic performance in propane DH (Tab. 1). Unfortunately, the binary carbide is less stable in the presence of H_2O (and CO_2) in the feed and partially decomposes into MoO_2, likely due to the higher oxophilicity of V. Thus, stable operation conditions can only be obtained in H_2-containing mixtures. Indeed the propylene productivity at 500°C, $C_3H_8/H_2/N_2$ = 1:2:1 and 5000 ml g^{-1} h^{-1} almost doubles from 10.2 to 18.0 μmol g^{-1} min^{-1} for the Mo_2C catalyst as the result of 8% V dopant, which can only in parts be explained by the slightly higher specific surface area (Tab. 2). As the apparent activation energy increases from 80 to 88 kJ mol^{-1} for Mo_2C and $(Mo_{0.92}V_{0.08})_2C$, respectively, this activity change must be referred to the generation of additional active sites, most likely associated with surface oxygen. Evidently, the oxycarbide provides a higher catalytic activity in propane DH than the pure carbide does.

Conclusion

The following picture of the active surface can be drawn (Fig. 7). The dehydrogenation reactions are independent of other reactions while CH_4 can be formed by hydrogenolysis of propane or propylene. Strong hydrogenolysis sites are defined as those that can activate C-C single bonds such as in propane, whereas weak sites are defined as those that can only activate propylene. This explains a disparity between the selectivity to ethylene/ethane and CH_4, which is seen in Fig. S2. Alkyl-recombinative sites leading to C_4 products can only be observed on the clean surface in high-vacuum. Based on the high-pressure XPS analysis and in close agreement with literature reports for bulk and supported MoC catalysts[4] we can ascribe the dehydrogenation pathways to the presence of residual oxygen in the carbide. This finding goes in parallel with more common Cr/Al_2O_3 or Pt-Sn/Al_2O_3 systems. As the reaction progresses at $\geq$ 500°C, the strong hydrogenolysis sites are deactivated by carbon deposition, which can serve as an additional source of CH_4 formation via methanation. At higher temperatures TPRC reveals that surface oxygen is stripped in the course of entire

carburization, leading to a loss of dehydrogenation sites. It means that the MoC system requires a delicate control of reaction parameters as surface carbon deposits cannot be removed by facile combustion in air. Instead, two strategies of stabilization of the selective sites have been proposed in the present work: (i) the addition of mildly oxidizing H_2O or CO_2 to the feed (the latter is rapidly converted to H_2O via rWGS), and (ii) the addition of V as an oxophilic dopant for the Mo_2C catalyst. However, still the optimization of process conditions require a balance between phase stability, coking, activity, and selectivity, which are all senstitive to the variation of reaction conditions.
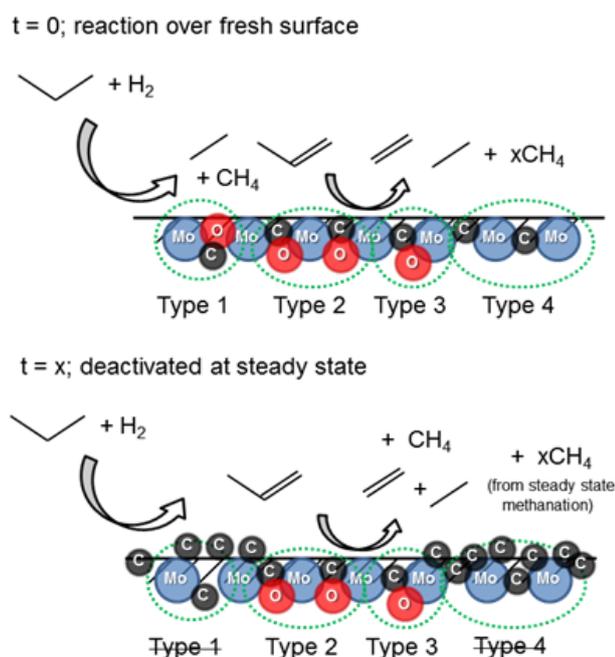
Figure 7. Propane reactivity over Mo_2C. Type 1 = alkyl-recombinative site; Type 2 = dehydrogenation site; Type 3 = weak hydrogenolysis site; Type 4 = strong hydrogenolysis site.

Moreover, this study proves that carbide phases of Mo and V are instable in the presence of H_2O or CO_2, which are typically present in high concentrations in the product stream of selective oxidation reactions, whereas stabilizing H_2 is absent here. Thus, a non-oxidative conversion in the oxygen-free regime via consecutive dehydrogenation pathways over such reduced catalyst states can be excluded.

Experimental Section

Catalyst preparation: Details of catalyst preparation as well as basic characterization is reported elsewhere.[15,32] Briefly, β-$Mo_{(1-x)}V_xO_3$ carbides were prepared by TPRC in 20% CH_4/H_2 in a rotary furnace with a maximum temperature of 675°C. After cooling, samples were passivated in 0.5% O_2/He, or transferred into a glove box before further processing.

Catalytic testing: The catalysts bed was fixed between two quartz wool plugs in the isothermal zone (± 0.5 K) of a U-shaped quartz reactor (inner diameter: 4 mm) located in a Carbolite furnace. The complete set-up is located in a heating box. All reactions were carried out over 295 mg catalyst mixed 1:1 by weight with SiC (sieve fraction 250-355 μm) with a total flow of 40 ml/min (WHSV: 8250 ml g^{-1} h^{-1}). Gas analysis is carried out with an Agilent 5890 GC equipped with FID for hydrocarbons and TCD for CO_2, O_2, N_2, CO, and H_2O.

Raman spectroscopy: Catalysts in the form of pressed wafers were *ex-situ* analyzed with a Horiba Jobin LABRAM microscope. All spectra were recorded for 60 s with the average of 3 accumulations at a magnification of 100X using an MPlan Olympus objective with an aperture value of 0.9. The light source was a 20 mW He-Ne laser with λ = 632.8 nm. *Quasi in situ* Raman spectra were obtained by the use of a custom designed SiO_2 cell. The sample was heated in a tube furnace under reaction conditions and periodically removed to record Raman spectra through a SiO_2 window.

X-ray photoelectron spectroscopy: Experiments were performed at the ISISS beamline at BESSY II synchrotron facility in Berlin. All samples were transferred without air contact. In situ measurements were performed at 0.3 mbar under flow conditions and the gas phase composition is monitored by QMS and GC. The sample is heated by a laser from the rear, which is incident on the stainless steel backing plate of the sample holder. *Ex situ* spectra were recorded at two positions on each sample. The Fermi edge was measured at each energy to correct for charging phenomena. Subtraction of a Shirley background and peak fitting was carried out using CasaXPS™ software. Gauss-Lorentzian peak shapes have been applied for peaks with oxidic character while a Doniach-Sunjic profile has been used for metallic components.

Transmission electron microscopy: TEM investigations were carried out with a Philips CM 200 FEG (Philips) equipped with a Gatan Image Filter (Gatan, Warrendale, PA) and a charge-coupled device (CCD) camera at 200 kV. HAADF-STEM and HRTEM investigations were carried out on a TITAN 80-300 (FEI) equipped with a Cs-corrector.

[1]   H. Böhm, *Electrochim. Acta* **1970**, *15*, 1273–1280.
[2]   R. B. Levy, M. Boudart, *Science* **1973**, *181*, 547–549.
[3]   F. Solymosi, R. Németh, *Catal. Lett.* **1999**, *62*, 197–200.
[4]   F. Solymosi, R. Németh, L. Óvári, L. Egri, *J. Catal.* **2000**, *195*, 316–325.
[5]   F. Solymosi, R. Németh, A. Oszkó, in *Stud. Surf. Sci. Catal.* (Ed.: J.. S. and T.H.F. E. Iglesia), Elsevier, **2001**, pp. 339–344.
[6]   M. J. Ledoux, F. Meunier, B. Heinrich, C. Pham-Huu, M. E. Harlin, A. O. I. Krause, *Appl. Catal. Gen.* **1999**, *181*, 157–170.
[7]   M. K. Neylon, S. Choi, H. Kwon, K. E. Curry, L. T. Thompson, *Appl. Catal. - Gen.* **1999**, *183*, 253–263.
[8]   M. E. Harlin, A. O. I. Krause, B. Heinrich, C. Pham-Huu, M. J. Ledoux, *Appl. Catal. Gen.* **1999**, *185*, 311–322.
[9]   H. Kwon, L. T. Thompson, J. Eng Jr., J. G. Chen, *J. Catal.* **2000**, *190*, 60–68.
[10]   M. Volpe, G. Tonetto, H. de Lasa, *Appl. Catal. Gen.* **2004**, *272*, 69–78.
[11]   B. M. Weckhuysen, R. A. Schoonheydt, *Catal. Today* **1999**, *51*, 223–232.
[12]   C. Yu, Q. Ge, H. Xu, W. Li, *Catal. Lett.* **2006**, *112*, 197–201.
[13]   J. Schäferhans, S. Gómez-Quero, D. V. Andreeva, G. Rothenberg, *Chem. – Eur. J.* **2011**, *17*, 12254–12256.
[14]   C. Bouchy, C. Pham-Huu, B. Heinrich, E. G. Derouane, S. B. Derouane-Abd Hamid, M. J. Ledoux, *Appl. Catal. Gen.* **2001**, *215*, 175–184.
[15]   T. Cotter, B. Frank, W. Zhang, R. Schlögl, A. Trunschke, *Chem. Mater.* **2013**, *25*, 3124–3136.
[16]   B. Frank, K. Friedel, F. Girgsdies, X. Huang, R. Schlögl, A. Trunschke, *ChemCatChem* **2013**, *5*, 2296–2305.
[17]   B. Frank, Z.-L. Xie, A. Trunschke, *Chem. Ing. Tech.* **2013**, *85*, 1290–1293.
[18]   F. E. Frey, W. F. Huppke, *Ind. Eng. Chem.* **1933**, *25*, 54–59.
[19]   J. J. H. B. Sattler, A. M. Beale, B. M. Weckhuysen, *Phys. Chem. Chem. Phys.* **2013**, *15*, 12095–12103.
[20]   T. Mongkhonsi, P. Prasertdham, A. Saengpoo, N. Pinitniyom, B. Jaikaew, *Korean J. Chem. Eng.* **1998**, *15*, 486–490.
[21]   A. Sadezky, H. Muckenhuber, H. Grothe, R. Niessner, U. Pöschl, *Carbon* **2005**, *43*, 1731–1742.
[22]   H. G. Karge, in *Stud. Surf. Sci. Catal.* (Ed.: E.M.F. and J.C.J. H. van Bekkum), Elsevier, **1991**, pp. 531–570.
[23]   O. Schwarz, B. Frank, C. Hess, R. Schomäcker, *Catal. Commun.* **2008**, *9*, 229–233.
[24]   A. Dinse, S. Khennache, B. Frank, C. Hess, R. Herbert, S. Wrabetz, R. Schlögl, R. Schomäcker, *J. Mol. Catal. Chem.* **2009**, *307*, 43–50.
[25]   D. Sanfilippo, I. Miracca, *Catal. Today* **2006**, *111*, 133–139.
[26]   T. A. (Xander) Nijhuis, S. J. Tinnemans, T. Visser, B. M. Weckhuysen, *Phys. Chem. Chem. Phys.* **2003**, *5*, 4361–4365.
[27]   F. Werfel, E. Minni, *J. Phys. C Solid State Phys.* **1983**, *16*, 6091–6100.
[28]   E. Minni, F. Werfel, *Surf. Interface Anal.* **1988**, *12*, 385–390.
[29]   P. C. Stair, *Langmuir* **1991**, *7*, 2508–2513.
[30]   G. H. Smudde Jr., P. C. Stair, *Surf. Sci.* **1994**, *317*, 65–72.
[31]   N. S. McIntyre, D. D. Johnston, L. L. Coatsworth, R. D. Davidson, J. R. Brown, *Surf. Interface Anal.* **1990**, *15*, 265–272.

[32] T. Cotter, The Reducibility of Mixed Mo/V Oxide Materials to Carbides and Their Reactivity in the Activation of Propane, Technische Universität Berlin, **2011**.
[33] B. E. Handy, J. A. Dumesic, R. D. Sherwood, R. T. K. Baker, *J. Catal.* **1990**, *124*, 160–182.
[34] R. Bacaud, P. Bussière, F. Figueras, *J. Catal.* **1981**, *69*, 399–409.
[35] J. F. Moulder, *Handbook of X-Ray Photoelectron Spectroscopy: A Reference Book of Standard Spectra for Identification and Interpretation of XPS Data*, Physical Electronics Division, Perkin-Elmer Corporation, **1992**.

7

t = 0; reaction over fresh surface
t = x; deactivated at steady state
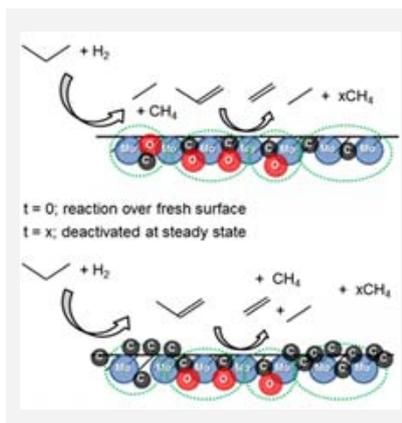
Black is beautiful: The active surface of mesoporous bulk molybdenum carbide catalysts during catalytic propane dehydrogenation sensitively responses to reaction conditions. The stable high performance catalyst is in a delicate balance between surface coking and irreversible bulk oxidation, which can be controlled by vanadium doping, reaction temperature, or by adding H_2, H_2O, or CO_2 to the feed.